Available online at www.sciencedirect.com
ScienceDirect
Journal of Power Sources 174 (2007) 442–448
JOURNAL OF POWER SOURCES
www.elsevier.com/locate/jpowsour

Hydrothermal synthesis of cathode materials

Jiajun Chen, Shijun Wang, M. Stanley Whittingham *

Institute for Materials Research, State University of New York at Binghamton, Binghamton, NY 13902, USA

Available online 22 July 2007

Abstract

A number of cathodes are being considered for the next generation of lithium ion batteries to replace the expensive $LiCoO_2$ presently used. Besides the layered oxides, such as $LiNi_yMn_yCo_{1-2y}O_2$, a leading candidate is lithium iron phosphate with the olivine structure. Although this material is inherently low cost, a manufacturing process that produces electrochemically active $LiFePO_4$ at a low cost is also required. Hydrothermal reactions are one such possibility. A number of pure phosphates have been prepared using this technique, including $LiFePO_4$, $LiMnPO_4$ and $LiCoPO_4$; this method has also successfully produced mixed metal phosphates, such as $LiFe_{0.33}Mn_{0.33}Co_{0.33}PO_4$. Ascorbic acid was found to be better than hydrazine or sugar at preventing the formation of ferric ions in aqueous media. When conductive carbons are added to the reaction medium excellent electrochemical behavior is observed.

Keywords: Olivine; Lithium battery; Rietveld analysis; Iron phosphate

1. Introduction

Critical to the success of new cathode materials, is their preparation, which controls the morphology, particle size and cation order amongst other critical parameters. Although traditionally high temperature methods have been used, they are both energy intensive and cannot readily produce many potentially metastable structures that might result in high lithium ion diffusivity. However, they do have the advantage of being hydroxyl/water free. There are many possible approaches to the synthesis of active materials, but in the end a commercially viable approach must be used [1]. Soft chemical approaches, such as hydrothermal/solvothermal or ion-exchange offer several advantages. Such methods are used on the tonnage quantities today, and so the chemical industry considers them viable. Hydrothermal synthesis has been extensively studied for simple oxides such as those of tungsten, molybdenum and vanadium, and today many of the key parameters are now understood [2]. Various phosphates have also been successfully prepared.

A cathode of particular interest is lithium iron phosphate, $LiFePO_4$, with the olivine structure [3]. This material is conventionally synthesized at elevated temperatures, but to take advantage of its low cost components it would be advantageous to use a low cost, low energy utilization synthesis approach. We originally showed in 2001 [4] that a range of iron phosphates could be synthesized at temperatures as low as 120 °C in just a few minutes. However, the lithium iron phosphate phase did not have a high capacity, which we later showed [5] was due to some lithium/iron disorder with around 7% iron on the lithium sites. As the structure has one-dimensional tunnels, any iron in the lithium tunnels will severely limit lithium insertion and removal. It is therefore essential to ensure complete ordering of the lithium and iron atoms. This orthormobic tunnel structure is compared with the tetragonal structure of lipscombite in Fig. 1; the latter has tunnels in two directions, and is less likely to be susceptible to tunnel blockage. However, although lithium-exchanged lipscombite shows excellent electrochemical behavior [6], the cell potential is more than 0.5 V lower than that of $LiFePO_4$ due to the reduction of the large inductive effect found in $LiFePO_4$.

We have therefore renewed our study of the hydrothermal process, in an attempt to understand the key parameters in the synthesis [7,8]. We have studied the effect of temperature, of reducing agent and of formation and/or addition of carbon conductors during the synthesis step. A key challenge in using aqueous solutions is to prevent the oxidation of ferrous to ferric. A reducing agent, such as hydrazine, has been used historically with mixed success in the formation of ferrous phosphates. We therefore explored this reductant and others such as ascorbic acid (vitamin C) and sugar for the hydrothermal formation of $LiFePO_4$. Another key challenge in using $LiFePO_4$ is to increase

* Corresponding author. Tel.: +1 607 777 4623; fax: +1 607 777 4623.
E-mail address: stanwhit@gmail.com (M.S. Whittingham).

0378-7753/$ – see front matter © 2007 Elsevier B.V. All rights reserved.
doi:10.1016/j.jpowsour.2007.06.189

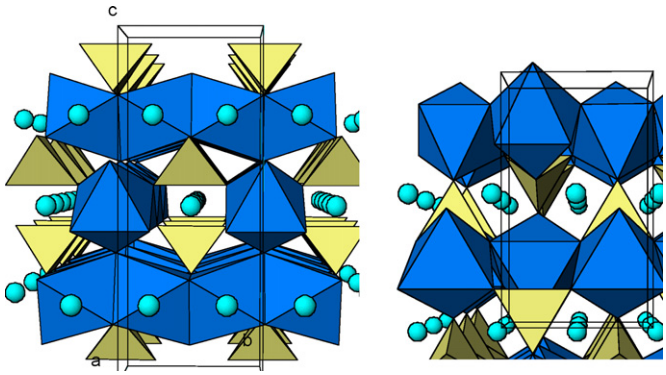

Fig. 1. Tunnel structures of (left) lipscombite, $Fe_{1.33}PO_4OH$, and (right) olivine, $LiFePO_4$, showing the FeO_6 octahedra, PO_4 tetrahedra, and the one-dimensional tunnels in which the lithium ions reside (from [7]).

the electronic and ionic conductivity. We therefore attempted to increase the conductivity of the product formed by incorporating carbon in the hydrothermal reaction medium either in solution as with ascorbic acid and sugar, or as carbon black or nanotubes.

2. Experimental

2.1. Ascorbic acid reductant

The $LiFePO_4$ was prepared by hydrothermal reaction in a Parr reactor as described previously. Specifically the starting materials were $FeSO_4{\cdot}7H_2O$ (98% Fisher), H_3PO_4 (85 wt.% solution Fisher), LiOH (98% Aldrich). The molar ratio of the Li:Fe:P was 3:1:1, and a typical concentration of $FeSO_4$ was 22 g l^{-1} of water. Sugar and/or l-ascorbic acid (99% Aldrich) was added as an in situ reducing agent to minimize the oxidation of ferrous to ferric, 1.3 g l^{-1} was used. Multi-Wall carbon nanotubes (95% Aldrich) were also added, 0.8 g l^{-1}. The autoclave was sealed and heated at 150–220 °C for 5 h.

For the $LiMnPO_4$ synthesis, $MnSO_4{\cdot}H_2O$ (98% Aldrich), H_3PO_4 (85 wt.% solution Fisher) and LiOH (98% Aldrich) with molar ratio 1:1:3 were dissolved in deionized water. The $MnSO_4$ and H_3PO_4 were mixed first, then 1.3 g l^{-1} l-ascorbic acid was added and after the addition of LiOH, a white gel formed in the beaker. The resulting gel was transferred into a 125 ml capacity Teflon-lined stainless steel autoclave. The autoclave was heated at 200 °C for 2 days. Precipitates were collected by suction filtration and dried at 60 °C for 3 h in a vacuum oven.

For the formation of $LiCoPO_4$, $CoSO_4{\cdot}7H_2O$ or $CoCl_2{\cdot}6H_2O$ was used as the Co^{2+} source; the molar ratio of the Li:Co:P was 3:1:1. 1.3 g l^{-1} l-ascorbic acid was added as reducing agent. The resulting pink gel was transferred into a 125 ml capacity Teflon-lined stainless steel autoclave. The autoclave was sealed and heated at 200 °C for 1 day. For the mixed metal phosphates the hydrothermal reaction was carried out at 200 °C for 2 days.

2.2. Hydrazine reductant

When using hydrazine as the reducing agent, 15 ml 1 M (~0.015 mol H_3PO_4) phosphoric acid was diluted to about 40 ml solution, then added about 1.25 ml 35 wt.% hydrazine (~0.015 mol, Hy1), 4.19 g ferrous sulfate 7-hydrate (~0.015 mol $FeSO_4$) powder was dissolved in this solution. Then a solution of 1.9 g lithium hydroxide monohydrate 30 ml water was added while constantly stirring for about 1 min; the pH of this mixture solution was 9.85. This mixture was then heated in a Teflon-lined autoclave at 200 °C for 6 h. In other preparations, extra phosphoric acid was added to adjust the pH, with most experiments at a starting value of 6.00. After hydrothermal reaction the pH value was 5.67.

2.3. Characterization

The electrochemical properties of the phosphates were examined using bag cells containing pure lithium as the anode, and Celgard™ as the separator at room temperature in a helium filled glove box. The cathodes were made by mixing 75 wt.% of the phosphate with 15 wt.% of carbon black and 10 wt.% of Teflon™ as the binder, and pressing into a stainless Exmet™ screen at 5 t pressure and 150–180 °C for 20–30 min. Typical cathode loading was 30–40 mg cm^{-2}. The electrolyte was 1 M $LiPF_6$ (lithium hexafluorophosphate) dissolved in a 1:1 volume ratio solution of ethylene carbonate (EC) and dimethyl carbonate (DMC) (EM Industries LP30). Cells were cycled galvanostatically using a MacPile II cycler.

X-ray powder diffraction data were collected on a Scintag XDS2000 θ-θ powder diffractometer equipped with a Ge(Li) solid state detector and Cu Kα sealed tube (λ = 1.54178 Å). Data were measured over the range of 5–80° 2θ with a step size of 0.02° and exposure of 5 s for routine characterization and over the range of 15–90° 2θ with a step size of 0.02° and exposure of 10 s for structure refinement; the samples were rotated. The Rietveld refinement of the X-ray powder diffraction patterns used the GSAS/EXPGUI package [9,10].

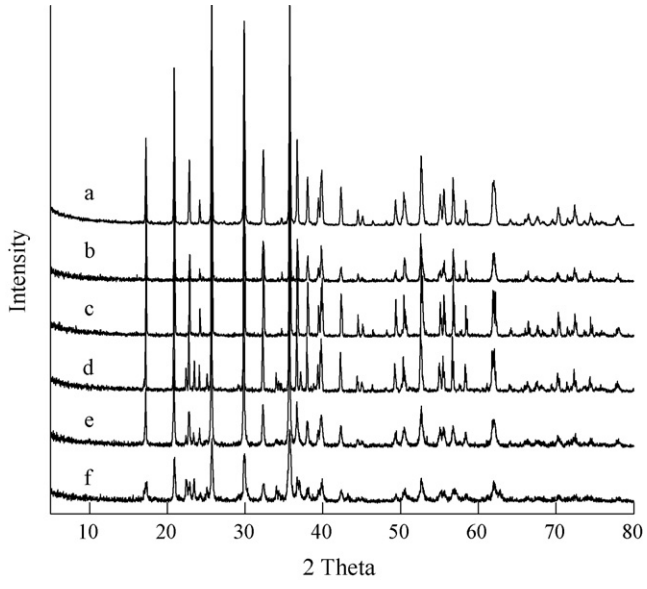

Fig. 2. X-ray diffraction patterns of $LiFePO_4$ formed in the presence of hydrazine and over a range of pH values. (a) No hydrazine, (b) pH 4 (c) pH 6, (d) pH 7 (e) pH 10, and (f) pH 10 with a 3:1 hydrazine:Fe ratio. All others had a 1:1 hydrazine ratio, and the pH was controlled by amount of phosphoric acid.

Scanning electron microscopy (SEM) data was collected on a Hitachi S-570 SEM. Prior to analysis, the sample was coated with 1:1 Au:Pd alloy in a Denton Vacuum Desk 1 sputter coater. The thermal gravimetric analysis was conducted on a TA2950 instrument under flowing oxygen at a heating rate of $5\,^{\circ}C\,min^{-1}$.

3. Results and discussion

3.1. Lithium iron phosphate produced in the presence of hydrazine

X-ray diffraction of the lithium iron phosphate formed in the presence of hydrazine showed an impurity phase when the pH was greater than around 7. This is apparent from an inspection of the data in Fig. 2, where extra diffraction lines can be observed between 20 and 25° 2θ in particular. In the absence of hydrazine no impurity phase was observed. In addition, Rietveld

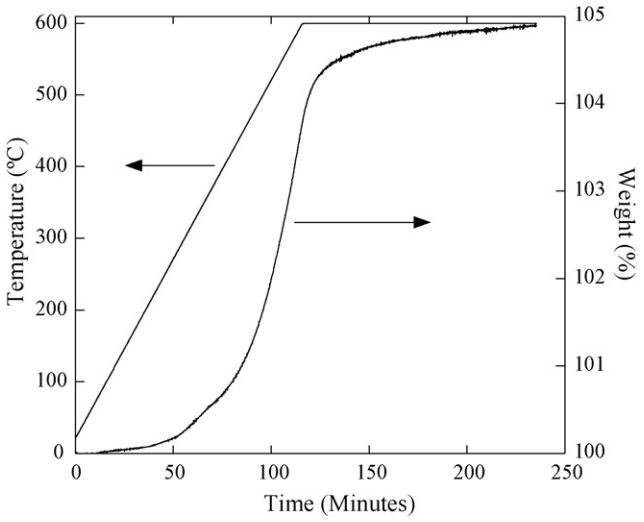

Fig. 3. Oxidation of $LiFePO_4$ formed at a pH value of 6. Heating rate was $5\,^{\circ}C\,min^{-1}$ to 600 °C, and the holding time at 600 °C was 2 h.

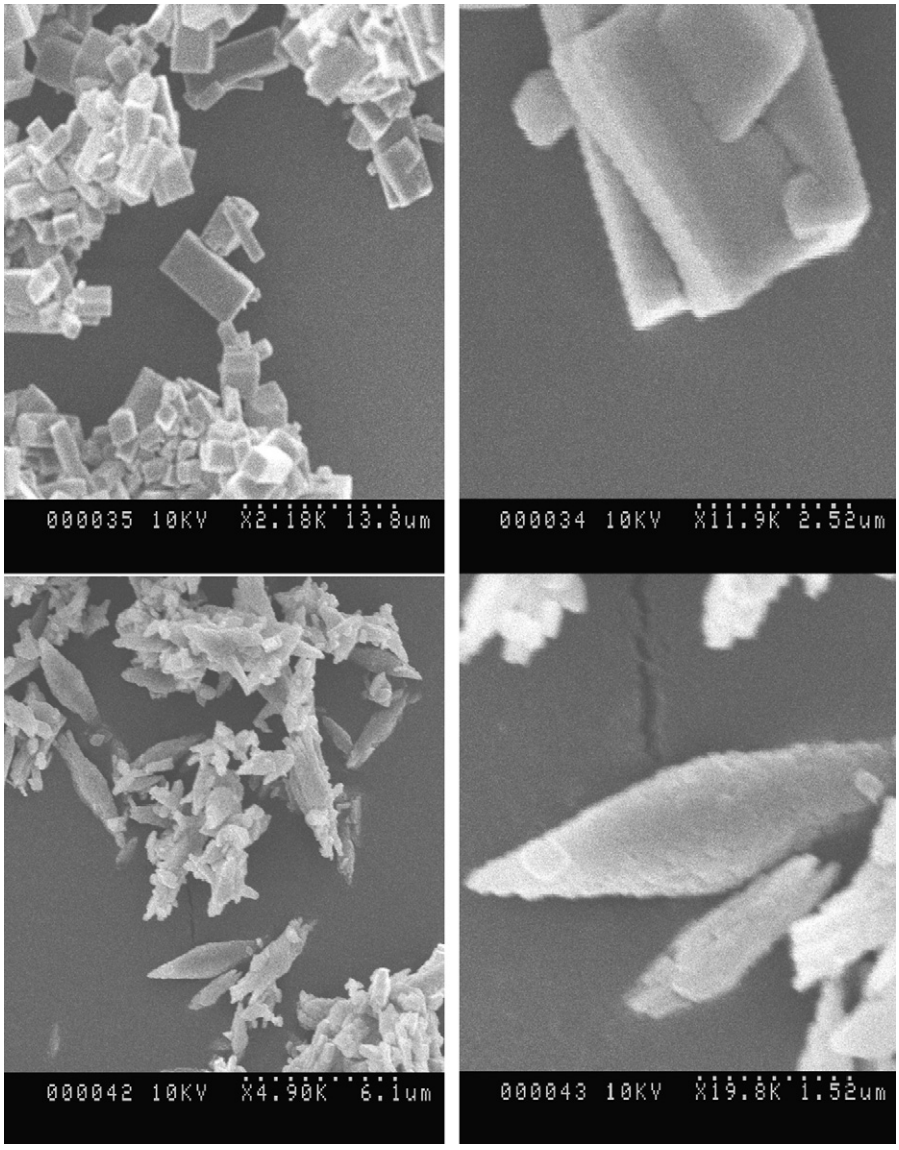

Fig. 4. SEM images of $LiFePO_4$ formed in the presence of hydrazine at pH values of 6 (top) and 10 (bottom) at two magnifications.

refinement of the X-ray data for the pH 6 and 10 samples showed 1.84% Fe on the Li sites for the latter but no Fe on the Li sites for the former. The cell parameters for the pH10 sample were $a = 10.333$ Å, $b = 5.998$ Å, $c = 4.695$ Å, and volume = 290.98 Å^3, for the pH 6 sample $a = 10.334$ Å, $b = 6.004$ Å, $c = 4.694$ Å, and volume = 291.24 Å^3; the latter is typical of that found for high temperature material [7]. Hence, subsequent work was performed at a pH of 6.

To determine the oxidation state of the iron, the $LiFePO_4$ was heated in oxygen to 600 °C, as shown in Fig. 3. The weight increase was over 4.9%, quite close to the expected value of 5.01% for a pure ferrous material. However, complete oxidation was only accomplished by holding the sample at 600 °C for 2 h. Normally, complete oxidation is achieved before 600 °C when the sample is heated at 5 °C min^{-1} [7]. The pH 10 samples oxidized much faster but only achieved a 3–4% weight gain, suggestive of the presence of a significant amount of ferric ions. This slow oxidation suggests a large particle size with slow ionic diffusion. This was confirmed by the SEM images of the material, which are shown in Fig. 4. The pH 6 sample has a rectangular block like morphology, several microns on a side and around 0.5 μm thick, quite a bit larger than the diamond-like morphology of the sample formed at a pH of 10 which is more typical of $LiFePO_4$ [4].

The electrochemical cycling of the pH 6 sample is shown in Fig. 5. Although the sample cycled well maintaining its capacity, its absolute capacity was much lower than the best hydrothermally prepared samples [7]. We have thus concluded that hydrazine is not an effective anti-oxidant for the synthesis of electrochemically active $LiFePO_4$.

3.2. Lithium iron phosphate produced in the presence of ascorbic acid

Our preliminary results [7] using ascorbic acid (vitamin C) showed the criticality of synthesis temperature and the presence of a reducing agent such as ascorbic acid. The $LiFePO_4$ compound crystallizes in the orthorhombic system with the tunnel structure shown in Fig. 1. Some transition metal is found in the lithium tunnel site displacing that lithium to the transition metal site. These transition metal ions block diffusion along the tunnels, potentially reducing the electrochemical capacity and the ultimate rate capability. A full Rietveld refinement of the X-ray diffraction patterns of the $LiFePO_4$ compounds was performed to determine the degree of cation mixing. The resulting data are shown in Fig. 6 and indicate that the metal disorder increases at lower synthesis temperatures approaching 8% at 120 °C, and dropping essentially to zero above 175 °C.

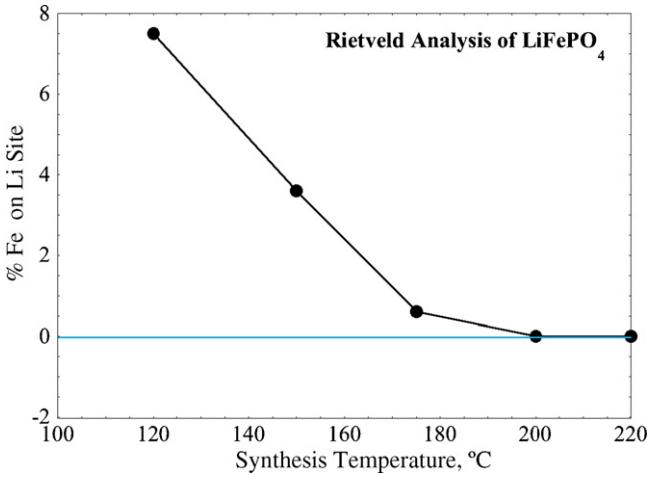

Fig. 6. The degree of cation mixing as a function of synthesis temperature, when ascorbic acid is present.

A challenge to the use of $LiFePO_4$ in batteries is the insulating behavior of the phosphate. This can be overcome by coating the particles with a conducting layer of for example carbon [11]. An attempt was therefore made to generate such a coating during the hydrothermal process. Ascorbic acid and sugar were added to the hydrothermal reactor, and a black product was formed as shown in Fig. 7. However, this material showed poor electrochemical behavior, with a capacity of only 90 mAh g^{-1}. This capacity did not fade on cycling. This could be due to several causes, such as sealing of the surface so that lithium removal could not occur, or that the carbon coating is essentially sp^3

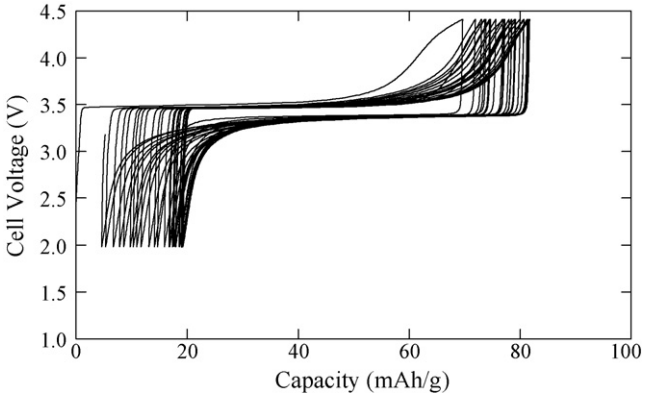

Fig. 5. Electrochemical cycling of the $LiFePO_4$ formed at a pH of 6. Cycling was performed between 4.4 and 2.0 V at a rate of 0.15 mA cm^{-2}.

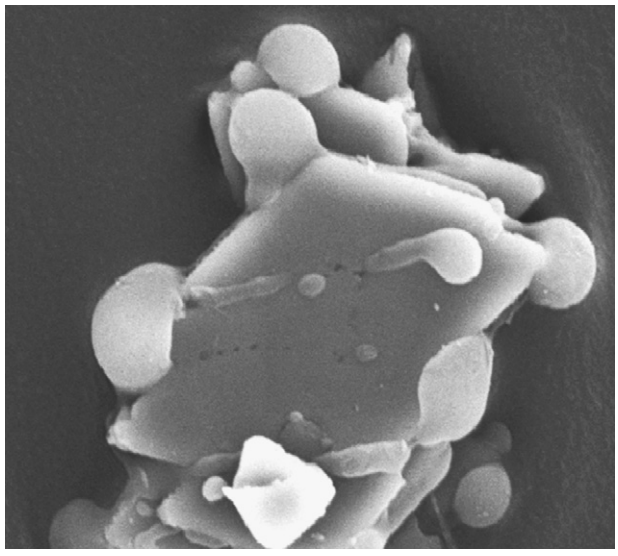

Fig. 7. The formation of a globular carbon coating on $LiFePO_4$ when an excess of ascorbic acid and sugar is added to the hydrothermal reactor.

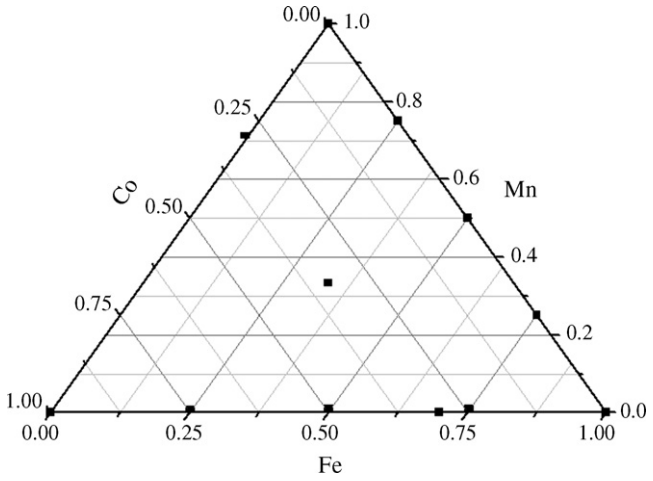

Fig. 8. Phase diagram showing some of the mixed cation phosphates synthesized hydrothermally.

carbon rather than the more conductive sp^2 carbon. The low carbonization temperature would suggest the likely formation of sp^3 carbon [12]. A Raman study of this sugar-coated sample indeed showed the presence of sp^3 carbon. This suggests that it may be difficult to chemically form a conducting carbon in situ at 200 °C. We therefore added conductive carbon in the form of carbon nanotubes to the hydrothermal reactor; the material formed showed the highest capacity, over 90% of theoretical, of any hydrothermal $LiFePO_4$ [8]. Thus, it is probably best to add the coating material in a conductive form to the hydrothermal reactor.

3.3. Other olivine lithium metal phosphates

We have studied the applicability of the hydrothermal process for olivines, $LiMPO_4$, other than the pure iron compound. A number of compounds, such as $LiFePO_4$, $LiMnPO_4$, $LiCoPO_4$, $LiNiPO_4$ and $LiMgPO_4$ are well known in the literature and in nature, but most have only been prepared at elevated temperatures. We have successfully formed a wide range of materials hydrothermally; some of these are shown in Fig. 8 for the compositions $Li(FeMnCo)PO_4$. The X-ray lattice parameters are shown in Table 1 together with the chemical composition and the Rietveld refinement; four typical powder patterns, with no impurities detected, are shown in Fig. 9. All these materials, synthesized at 200 °C, showed no lithium–metal (M) mixing.

Table 1
Lattice constants of hydrothermal phosphates

Composition, $LiMPO_4$ (M=)	A (Å)	B (Å)	c (Å)	Vol. (Å^3)	R_p (%)
Fe	10.332	6.005	4.693	291.23	10.5
$Fe_{0.75}Mn_{0.25}$	10.375	6.035	4.711	294.99	11.1
$Fe_{0.5}Mn_{0.5}$	10.399	6.053	4.723	297.30	11.5
$Fe_{0.25}Mn_{0.75}$	10.435	6.078	4.742	300.77	12.3
Mn	10.468	6.104	4.755	303.89	10.4
Co	10.215	5.918	4.706	284.49	5.1
$Fe_{0.7}Co_{0.3}$	10.297	5.982	4.697	289.33	9.6
$Fe_{0.33}Mn_{0.33}Co_{0.33}$	10.337	6.008	4.717	292.92	10.7
$Mg_{0.25}Fe_{0.75}$	10.296	5.980	4.694	289.37	15.2
$Fe_{0.99}Al_{0.01}$	10.345	5.999	4.703	291.87	10.8
$Fe_{0.95}V_{0.05}$[a]	10.349	6.001	4.708	292.41	19.5

[a] A vanadium phosphate phase was also found, so the doping level in the olivine structure is less than the nominal 5%; this impurity also explains the high value of R_p.

The cell unit volumes change as expected from the $LiFePO_4$ with the change in size of the metal M ion. Thus, there appears to be complete solubility for the ions Fe, Mn and Co; magnesium also appears to be soluble over the whole range for $LiFe_{1-y}Mg_yPO_4$. We are presently investigating the $LiMn_{1-y}Mg_yPO_4$ to determine the solubility range, and to see if

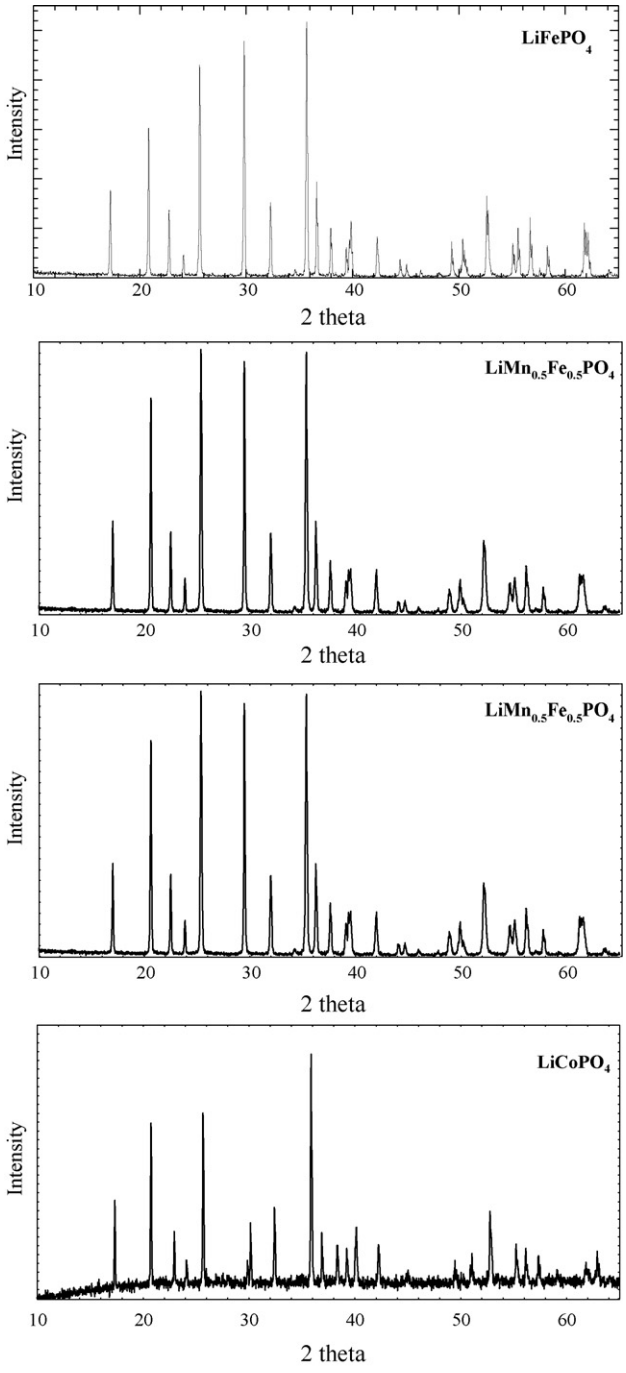

Fig. 9. X-ray diffraction patterns of (from top) $LiFePO_4$, $LiFe_{0.5}Mn_{0.5}PO_4$, $LiMnPO_4$, and $LiCoPO_4$.

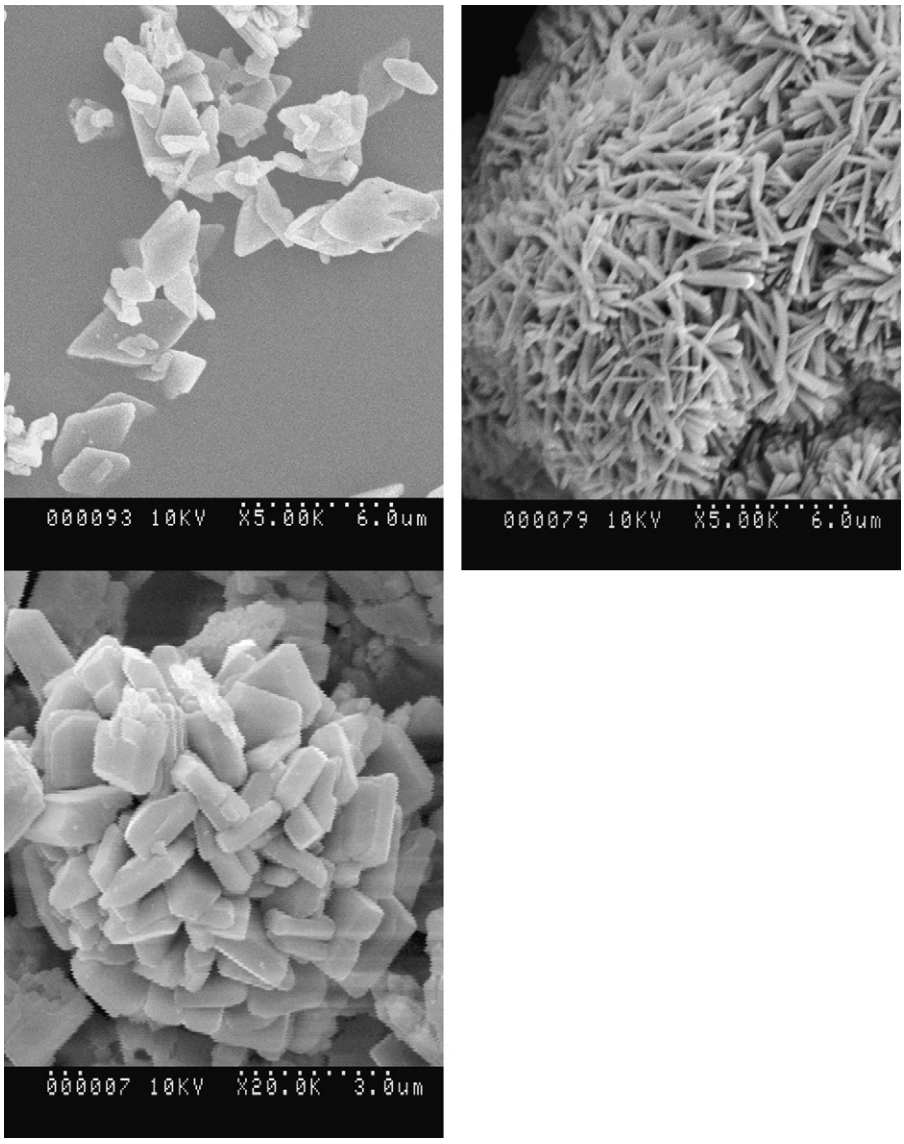

Fig. 10. Morphology of (top left) $LiFePO_4$ compared with (top right) $LiMnPO_4$ and (bottom left) $LiFe_{0.5}Mn_{0.5}PO_4$.

the advantages found for magnesium substitution in the $LiFePO_4$ compound can be extended to $LiMnPO_4$ allowing it to cycle over the full range of composition.

Attempts to form $LiNiPO_4$ using the same hydrothermal approach resulted in the formation of $Ni_{12-\delta}(HPO_3)_8(OH)_6$, Rietveld refinement of its powder X-ray diffraction showed it to be hexagonal, *P*63*mc* space group. The cell parameter were $a = 12.5307(9)$ Å, $c = 4.9548(4)$ Å, cell volume = 673.767 Å3. The reliability factor R_p was 7.2%; the site occupancy for the nickel ion is 0.917 suggesting significant vacancies on the nickel site, with only around 11 nickel atoms in one unit cell as previously reported [13].

Single crystals of NH_4FePO_4 monohydrate were made at 170 °C on reacting ammonia, ferrous sulfate, and phosphoric acid. Preliminary powder X-ray diffraction analysis was done by Rietveld refinement. This material is orthorhombic, *Pmn*21 space group, with lattice parameter $a = 5.654(6)$ Å, $b = 8.936(2)$ Å, and $c = 4.805(8)$ Å.

The morphology of the olivines formed depends greatly on their chemical composition as shown in Fig. 10. Thus $LiFePO_4$ tends to form as diamond shape platelets that are typically a 100 nm thick and 1–3 μm on an edge. In contrast $LiMnPO_4$ forms as a matted cluster of rods, about 3 μm long, and several hundred nm in diameter; the spherical clusters are about 25–40 μm in diameter. The mixed iron manganese compound forms a more block morphology. We are presently investigating the impact of the morphology on the electrochemical properties.

4. Conclusions

Hydrothermal synthesis is a powerful method for the formation of cathode materials, and can be successfully used to form a wide range of olivine-structured materials. These may contain a single metal ion, or a mixture. Ordering of the lithium and metal ions can be obtained by performing the synthesis above 175 °C. Ascorbic acid has been found to be an effective agent to mini-

mize oxidation of ferrous to ferric in the aqueous solutions used. The addition of carbon nanotubes to the hydrothermal reactor gave $LiFePO_4$ with excellent electrochemical behavior.

Hydrothermal synthesis leads to well-crystalline material with particle size generally in the micron size, and with a thickness of a few hundred nanometers; fortunately the short dimension is the diffusion direction. Even larger crystals can be formed suitable for in situ studies of phase changes and diffusion studies [14], and the use of high concentration ascorbic acid and polyethylene glycol leads to the formation of single crystals up to a mm in size [15]. The present challenge is to form nanosize particles with conductive coatings under hydrothermal conditions; there is some evidence that smaller particles of size 0.3–1 μm can be formed by a modified hydrothermal process [16].

Acknowledgements

We thank the US Department of Energy, Office of FreedomCAR and Vehicle Technologies, for their financial support through the BATT program at LBNL.

References

[1] M.S. Whittingham, in: G.A. Nazri (Ed.), Lithium Batteries, Kluwer, 2003.
[2] T.A. Chirayil, P.Y. Zavalij, M.S. Whittingham, Chem. Mater. 10 (1998) 2629.
[3] A.K. Padhi, K.S. Nanjundaswamy, J.B. Goodenough, J. Electrochem. Soc. 144 (1997) 1188.
[4] S. Yang, P.Y. Zavalij, M.S. Whittingham, Electrochem. Commun. 3 (2001) 505.
[5] S. Yang, Y. Song, P.Y. Zavalij, M.S. Whittingham, Electrochem. Commun. 4 (2002) 239.
[6] Y. Song, P.Y. Zavalij, N.A. Chernova, M.S. Whittingham, Chem. Mater. 17 (2005) 1339.
[7] M.S. Whittingham, Y. Song, S. Lutta, P.Y. Zavalij, N.A. Chernova, J. Mater. Chem. 15 (2005) 3362.
[8] J. Chen, M.S. Whittingham, Electrochem. Commun. 8 (2006) 588.
[9] B.H. Toby, J. Appl. Crystallogr. 34 (2001) 210.
[10] A.C. Larson, R.B. VonDreele, General structure analysis system (GSAS), Los Alamos Natl. Lab. Rep. LAUR 86 (2000), 748.
[11] N. Ravet, J.B. Goodenough, S. Besner, M. Simoneau, P. Hovington, M. Armand, Electrochem. Soc. Abstr. 99–2 (1999) 127.
[12] M.M. Doeff, Y. Hu, F. McLarnon, R. Kostecki, Electrochem. Solid-State Lett. 6 (2003) A207.
[13] M.D. Marcos, P. Amoros, A. Beltran-Porter, R. Martinez-Manez, J.P. Attfield, Chem. Mater. 5 (1993) 121.
[14] G. Chen, X. Song, T.J. Richardson, Electrochem. Solid-State Lett. 6 (2003) A207.
[15] J. Chen, M.J. Vacchio, S. Wang, N. Chernova, P.Y. Zavalij, M.S. Whittingham, submitted for publication.
[16] M. Eisgruber, L. Wimmer, G. Nuspl, Canadian Patent CA2537278 (2005).